Journal of Magnetism and Magnetic Materials 335 (2013) 125–130

Contents lists available at SciVerse ScienceDirect

Journal of Magnetism and Magnetic Materials

journal homepage: www.elsevier.com/locate/jmmm

Permeability analysis of magnetic alloy thin films in inductance transmission line

Masakatsu Senda*

Department of Electrical and Computer Engineering, Oyama National College of Technology, 771 Nakakuki, Oyama, Tochigi 323-0806, Japan

ARTICLE INFO

Article history:
Received 3 December 2012
Received in revised form
25 January 2013
Available online 11 February 2013

Keywords:
Permeability
Magnetic alloy thin film
Transmission line

ABSTRACT

This article reports on a complex permeability ($\mu_r=\mu_r'-j\mu_r''$) analysis in the range from 50 MHz to 13.5 GHz of magnetic alloy thin films in an inductance transmission line (ITL). The ITL has shell-type closed magnetic circuit structures composed of magnetic films and a conductive line, and the reflection (Γ) and transmission (T) are measured with a two-port method. μ_r'' is estimated from Γ and T by analyzing multiple reflections in the ITL, and μ_r' is obtained using the Kramers–Kronig relation. The μ_r-f characteristics for Co–Fe film are confirmed to be in relatively good agreement with results from an impedance measurement and with coupled Landau–Lifschitz and eddy current theories. The applicable conditions of this technique are discussed, and the requirements $\mu_{rs}' \ll \sim 2500$ and $\mu_{rs}' f_k \ll \sim 6500$ GHz are derived.

1. Introduction

High-performance micro-magnetic devices, for example, thin film magnetic heads, inductors, transformers, and filters, are required for high-density magnetic recording and high-speed signal processing in electronic equipments. These applications inevitably have required the developments of superior soft-magnetic alloy films and of complex permeability measurement techniques which work in the gigahertz range. In the past, the coil method, which employs drive and pick-up coils [1,2], was often used as a measurement technique, but its measurement frequency was limited by resonance phenomena in the coils. The cavity method, where permeability is estimated from shifts of the Q-value and resonance frequency, is also well known, but this works only at discrete frequencies. The techniques for measuring in continuous frequencies above the gigahertz range include two-port measurement methods with strip or microstrip lines [3–6], one-port methods with coaxial lines [7–10], and one-port methods with single coils or strip lines [11–14]. These measurements require accurate setup, calibrations, and error corrections. On the other hand, a permeability measurement using an inductance transmission line (ITL) was investigated [15]. This is a type of two-port method, and it estimates the permeability from the transmission characteristics of the ITL. In this technique, the ITL has to be formed into a thin film device, and it is only the imaginary part of the permeability that can be directly obtained from the experimentally measured values. However, the transmission characteristics of the ITL have not been analyzed enough, and a detailed understanding of the characteristics would be helpful for examining the permeability measurement technique for microfabricated magnetic alloy thin films and the technique in the higher frequency range. In this paper, first, multiple reflections in the ITL were analyzed and the permeability was estimated. Next, the estimated permeability was compared with values given by coupled Landau–Lifschitz and eddy current theories [16]. Finally, the applicable conditions of this technique were studied.

2. Sample preparation

The ITL is shown in Fig. 1. Sputtering and photolithographic techniques were used to make it. The ITL was composed of a conductive line and magnetic alloy thin films which sandwiched the conductive line from above and below on a glass substrate with a ground. The substrate was 0.5 mm-thick, and its dielectric constant was 1.52. The magnetic films were formed into strips, and they had shell-type closed magnetic circuit structures. The dimensions were $l_c=10$ mm, $l_m=w_c=1500$ μm, $w_m=d_c=50$ μm, $t_c=2$ μm, $d_m=5$ μm. Cu film was used for the conductive line. For the magnetic films, 50 nm-thick $Co_{50}Fe_{50}$ (at.%: permendur) alloy layers (ten layers) were multilayered with 100 nm-thick SiO_2 layers (nine layers), and the net magnetic film thickness (t_m) was 0.5 μm. The film thicknesses were measured by using the Talystep method. The thicknesses were controlled by the sputtering times based on the preliminarily obtained deposition rates. This

* Tel.: +81 285 20 2243.
E-mail address: senda@oyama-ct.ac.jp

0304-8853/$ - see front matter © 2013 Elsevier B.V. All rights reserved.
http://dx.doi.org/10.1016/j.jmmm.2013.02.002

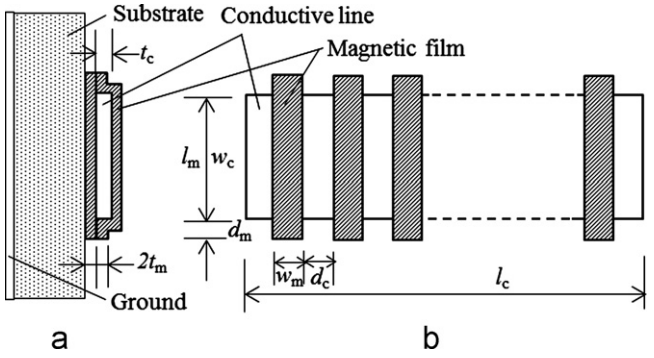

Fig. 1. Schematic diagram of inductance transmission line (ITL): (a) cross-section and (b) top view.

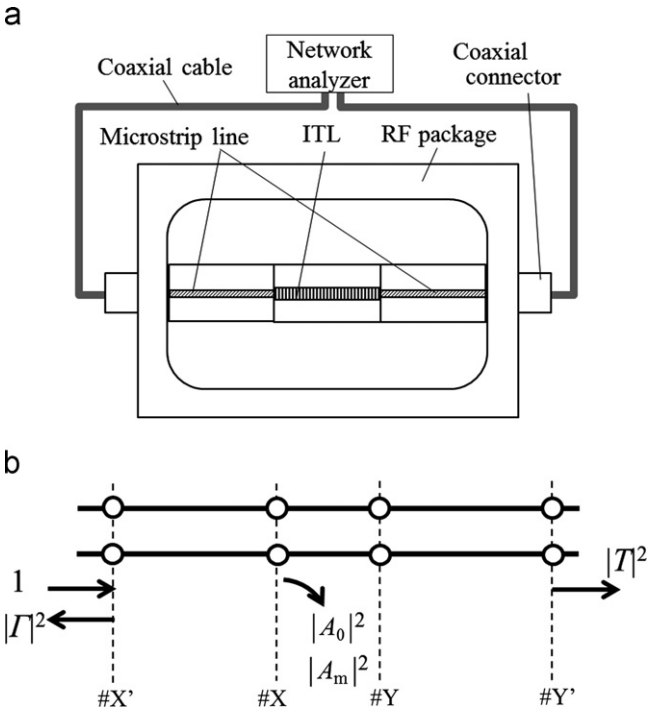

Fig. 2. ITL installed in RF package: (a) top view and (b) equivalent circuit.

technique was reproducible, and error in the thicknesses was about ±5%. The Co–Fe film exhibited a saturation magnetization (M_s) of 1950 kA/m, an electric resistivity (ρ) of $20\times10^{-8}\,\Omega\,m$, and a saturation magnetostriction (λ_s) of $\sim+10^{-4}$. An uniaxial anisotropy field (H_k) of 16 kA/m was generated through the inverse magnetostrictive effect, in which H_k is expressed by $\sim\sigma_f\lambda_s/M_s$. The compressive film stress (σ_f) was $\sim-10^2$ MPa, and the magnetization easy axis was parallel to the short length direction of the magnetic film strips. An external magnetic field (H_{ex}) of several tens of kiloampere per meter was applied in the long length direction of the strips in order to remove the magnetic films contribution from the ITL. The above closed magnetic circuit structure and the strip shape made the demagnetizing field in the long length direction negligible.

Fig. 2(a) shows the top view of the ITL installed in an RF package, and Fig. 2(b) shows the equivalent circuit. The ITL was joined to microstrip lines by soldering at the #*X* and #*Y* planes in the package. The transmission characteristics of the ITL were measured in the frequency range from 50 MHz to 13.5 GHz using a network analyzer. The calibration reference planes for reflection and transmission were the #*X*′and #*Y*′ planes in Fig. 2(b). The characteristic impedances for the network analyzer, coaxial cables, coaxial connectors, and the microstrip lines were set at 50 Ω. An HP8719C network analyzer and an HP4191A impedance meter were used for the measurements.

3. Results and discussion

3.1. Experimental analysis

In this section, the magnetic loss ($|A_m|^2$) due to the magnetic films is analyzed using the transmission characteristics of the ITL, and the imaginary part (μ_r'') of the complex permeability ($\mu_r=\mu_r'-j\mu_r''$) is estimated from $|A_m|^2$ at each frequency (f). The real part (μ_r') is calculated from the $\mu_r''-f$ characteristics using the Kramers–Kronig (K–K) relation [17].

$|A_m|^2$ can be described using the reflection (Γ) and transmission (T) coefficients. In Fig. 2(b), $|\Gamma|^2$, $|T|^2$, $|A_m|^2$, and ($|A_0|^2$), which includes the losses other than magnetic loss, have the following relation:

$$|T|^2=\left(1-|\Gamma|^2\right)\left(1-|A_0|^2\right)\left(1-|A_m|^2\right) \tag{1}$$

Here, H and 0 represent states with and without H_{ex}. $|A_0(H)|^2$ is equal to $|A_0(0)|^2$ because A_0 is magnetic-independent, and $|A_m(H)|$ can be set at nearly zero because the magnetic films should be saturated by applying H_{ex}. M is defined as $(1-|\Gamma|^2)/|T|^2$. The following relation is derived:

$$|A_m(0)|^2=1-M(H)/M(0) \tag{2}$$

The relation between $|A_m(0)|^2$ and μ_r'' can be examined by analyzing multiple reflections in the ITL. The multiple reflection model is shown in Fig. 3. In general, reflections would occur at junctions because of differences in connector types and propagation modes even if the characteristic impedances are matched. So, complicated reflections are also thought to occur at the junctions in the actual circuit shown in Fig. 2(a). In this study, the circuit was simplified into a model [18] with two reflecting planes of #*X* and #*Y*, as shown in Fig. 3. The characteristic impedances are Z_0 for the #1 and #3 sections and Z_{ci} for the #2 section. Reflections (Γ_i: $i=1, 2, 3$) and transmissions (T_{ij}: $i=1, 2, 3, j=1, 2$) at the #*X* and #*Y* planes are defined as shown in Fig. 3. The total reflection (Γ) at #*X* and total transmission (T) from #1 to #3 correspond to the Γ and T in Eq. (1), respectively. Γ and T are modified using the relations, $\Gamma_3=\Gamma_2=-\Gamma_1$, $T_{12}=1-\Gamma_1$, $T_{21}=1+\Gamma_1$, and $T_{32}=1+\Gamma_3$, as follows:

$$\begin{aligned}\Gamma&=\Gamma_1+T_{12}\Gamma_3T_{21}\exp(-2\gamma x)[1+(\Gamma_2\Gamma_3\exp(-2\gamma x))+(\Gamma_2\Gamma_3\exp(-2\gamma x))^2+\cdots]\\&=\Gamma_1+T_{12}\Gamma_3T_{21}\exp(-2\gamma x)/(1-\Gamma_2\Gamma_3\exp(-2\gamma x))\\&=\Gamma_1(1-\exp(-2\gamma x))/(1-\Gamma_1{}^2\exp(-2\gamma x))\end{aligned} \tag{3}$$

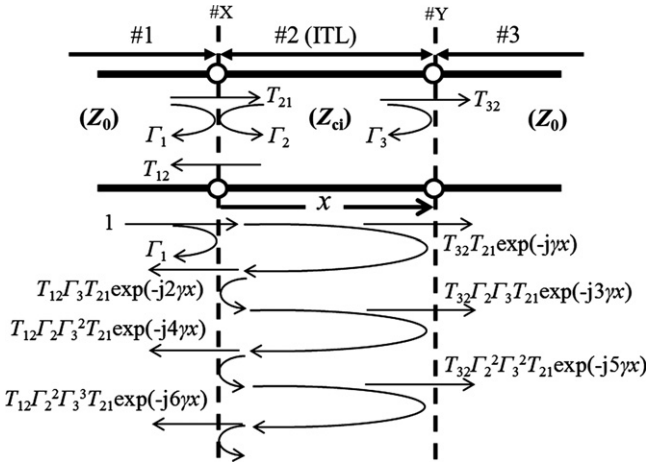

Fig. 3. Model of multiple reflections.